

AFWAL-TR-83-2095

WAVE ENGINE TECHNOLOGY DEVELOPMENT

Richard R. Coleman

GENERAL POWER CORPORATION
225 PLANK AVENUE
PAOLI, PENNSYLVANIA 19301

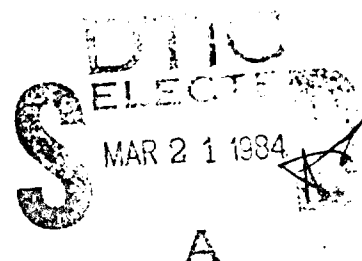


JANUARY 1984

FINAL REPORT FOR PERIOD MAY - SEPTEMBER 1983

APPROVED FOR PUBLIC RELEASE; DISTRIBUTION UNLIMITED

AERO PROPULSION LABORATORY
AIR FORCE WRIGHT AERONAUTICAL LABORATORIES
AIR FORCE SYSTEMS COMMAND
WRIGHT-PATTERSON AIR FORCE BASE, OHIO 45433



DTIC FILE COPY

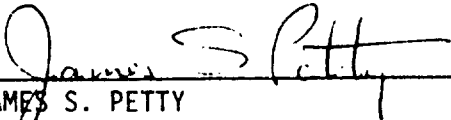
84 03 20 006

NOTICE

When Government drawings, specifications, or other data are used for any purpose other than in connection with a definitely related Government procurement operation, the United States Government thereby incurs no responsibility nor any obligation whatsoever; and the fact that the government may have formulated, furnished, or in any way supplied the said drawings, specifications, or other data, is not to be regarded by implication or otherwise as in any manner licensing the holder or any other person or corporation, or conveying any rights or permission to manufacture use, or sell any patented invention that may in any way be related thereto.

This report has been reviewed by the Office of Public Affairs (ASD/PA) and is releasable to the National Technical Information Service (NTIS). At NTIS, it will be available to the general public, including foreign nations.

This technical report has been reviewed and is approved for publication.

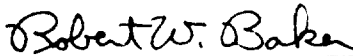


JAMES S. PETTY
Project Engineer



ERIK W. LINDNER
Technical Area Manager

FOR THE COMMANDER



ROBERT W. BAKER, Major, USAF
Deputy Director
Turbine Engine Division
Aero Propulsion Laboratory

"If your address has changed, if you wish to be removed from our mailing list, or if the addressee is no longer employed by your organization please notify AFMNL/POTA, W-PAFB, OH 45433 to help us maintain a current mailing list".

Copies of this report should not be returned unless return is required by security considerations, contractual obligations, or notice on a specific document.

UNCLASSIFIED

SECURITY CLASSIFICATION OF THIS PAGE

REPORT DOCUMENTATION PAGE

1a. REPORT SECURITY CLASSIFICATION UNCLASSIFIED		1b. RESTRICTIVE MARKINGS	
2a. SECURITY CLASSIFICATION AUTHORITY		3. DISTRIBUTION/AVAILABILITY OF REPORT Approved for public release. Distribution Unlimited	
2b. DECLASSIFICATION/DOWNGRADING SCHEDULE			
4. PERFORMING ORGANIZATION REPORT NUMBER(S)		5. MONITORING ORGANIZATION REPORT NUMBER(S) AFWAL-TR-83-2095	
6a. NAME OF PERFORMING ORGANIZATION General Power Corp	6b. OFFICE SYMBOL (If applicable)	7a. NAME OF MONITORING ORGANIZATION AFWAL/POTA	
6c. ADDRESS (City, State and ZIP Code) 225 Plank Ave Paoli PA 19301		7b. ADDRESS (City, State and ZIP Code) Wright-Patterson AFB OH 45433	
8a. NAME OF FUNDING/SPONSORING ORGANIZATION DARPA	8b. OFFICE SYMBOL (If applicable) TTO	9. PROCUREMENT INSTRUMENT IDENTIFICATION NUMBER F33615-83-C-2326	
8c. ADDRESS (City, State and ZIP Code) 1400 Wilson Blvd Arlington VA 22209		10. SOURCE OF FUNDING NOS.	
11. TITLE (Include Security Classification) Wave Engine Technology Development		PROGRAM ELEMENT NO. 52301E	PROJECT NO. DARPA
		TASK NO. 83	WORK UNIT NO. 01
12. PERSONAL AUTHOR(S) Coleman, Richard R.			
13a. TYPE OF REPORT Final	13b. TIME COVERED FROM May 83 TO Sep 83	14. DATE OF REPORT (Yr., Mo., Day) January 1984	15. PAGE COUNT 21
16. SUPPLEMENTARY NOTATION			
17. COSATI CODES		18. SUBJECT TERMS (Continue on reverse if necessary and identify by block number)	
FIELD	GROUP	SUB. GR.	
20	13, 14		
21	01		
		Wave Compression, Expansion; Wave Turbine Wave Engine	
19. ABSTRACT (Continue on reverse if necessary and identify by block number) Self Sustaining operation of the GPC Wave Engine Demonstration Unit (DU) was obtained in the range of 6500 to 8000 rpm using wave rotors with nozzle-to-chamber area ratios (A ₂ /A ₁) of .44 and .50. One test data run is compared in detail with the corresponding data from the GPC Wave Engine Simulation Program. Seal development during the contract period resulted in the design and preliminary test of a self-servoed face seal for the high pressure air port of the DU. Also, mechanically attached radial strip seals of inhibited graphite proved to be very effective in controlling angular leadage within the wave rotor cavity.			
20. DISTRIBUTION/AVAILABILITY OF ABSTRACT UNCLASSIFIED/UNLIMITED <input checked="" type="checkbox"/> SAME AS RPT <input type="checkbox"/> DTIC USERS <input type="checkbox"/>		21. ABSTRACT SECURITY CLASSIFICATION UNCLASSIFIED	
22a. NAME OF RESPONSIBLE INDIVIDUAL ERIK W. LINDNER		22b. TELEPHONE NUMBER (Include Area Code) (513) 255-4830	22c. OFFICE SYMBOL AFWAL/POTA

DD FORM 1473 83 APR

EDITION OF 1 JAN 73 IS OBSOLETE.

UNCLASSIFIED
SECURITY CLASSIFICATION OF THIS PAGE

SUMMARY

During the period covered by this report, all items in the work statement (Reference 2) were completed. As an added bonus, the development work on the face seals resulted in such improved performance by the GPC Demonstration Unit (DU) that self-sustaining power without external assistance was achieved using both Rotor "B" and Rotor "A".

Rotor "A" is aerodynamically cleaner than Rotor "B" and also has a higher value of rotor nozzle-to-chamber area ratio (A_z/A_y in the usual terminology—see Ref. 1) by some 12%. The more open rotor nozzle contributes to an improved circulation of high pressure air in the combustor loop, thus permitting higher fuel flow for a given combustor gas exit temperature (T_{05}). The experimental results also correlate with very small deviation from the results predicted by the GPC Wave Engine Computer Simulation as indicated by Table 1.

Seal Development. Two types of face seals were designed and used during the tests.

One of these (see Figure 3) is a servo-type seal which is located between the High Pressure Air Port and the Exhaust Port. It contains two seal elements made of graphite-filled polyimide plastic. One of these, the pilot seal, operates in a region of near zero angular pressure gradient and senses the axial proximity of the wave rotor blades. It then acts to position the main seal, located at the leading edge of the High Pressure Air Port, to some prescribed axial distance from the rotor. Servo energy is supplied by the high pressure air. This seal will be the subject of a patent application by GPC as prescribed in the pertinent contract clause.

Other experiments were conducted using mechanically attached radial strip seals fabricated from oxidation inhibited graphite. These seals were used in place of the thermally sprayed nickel-graphite abradable material. The latter was generally unsatisfactory for the rotor blade annulus seals because of damage inflicted upon the wave rotor in the event of rubbing at high speeds. The inhibited graphite is also apparently more resistant to erosive action of the gases than is abradable material.

The two-element servo-type seals show promise of being very effective and nearly nonwearing. The design of the present seal is not optimal by any means because it was necessary to work within the constraints of the existing DU port face hardware. It would be necessary to redesign the High Pressure Air Port face and diffuser in order to accommodate an improved seal configuration and servo system.

The surround seals, i.e., the stator seals surrounding the wave rotor shroud, are flame sprayed using a nickel-graphite material, and then machined to the proper diameter. At combustor gas temperatures approaching 1700 F. these seals tend to erode slowly and thus do not appear to be useful near the hot gas ports of high performance wave engines. There are other solutions to this particular seal problem, however. GPC has already made preliminary designs of seals which would be very desirable and effective in this location.

GPC Wave Engine Computer Simulation Program

There are still certain tasks which must be accomplished before the transfer of this rather complex program to the new microcomputer is complete. However, the bulk of this work has been completed and the program has been used successfully as evidenced by the data presented throughout this report.

This is a large finite element type program containing several thousand lines of code as compiled. It is capable of solving the internal wave and flow dynamics of a rotor with defined geometry running between sidewalls in which are located ports that are compatible with the blade height of the rotor but arbitrary with respect to length, location, and physical entrance or exit angles. Any port can be designated as an inlet or as an outlet port. The computations can be made on an open loop basis for arbitrary stagnation conditions at the plane of the inlet ports and arbitrary static conditions in the plane of the exit ports. In this case, all port flows and state conditions as well as the final wave field on the rotor are calculated both as detailed regions and as bulk or mixed conditions. If two ports are interconnected, then the computation can be iterated by loop balancing procedures until mass flow and other specified conditions are satisfied.

The simulations have been used principally to predict the performance of the GPC DU using Rotor "A" ($A_z/A_v = .50$) because Rotor "B" ($A_z/A_v = .44+$) was repaired after most of the blade joints broke as a result of inadequate control by the vendor of the furnace brazing process. The necessary repairs degraded the aerodynamic performance and reduced the nozzle-to-chamber area ratio from 0.50 to approximately 0.44. These deficiencies made it difficult, and certainly not worthwhile, to measure flow path imperfections and incorporate them into the rotor blade configuration file of the computer simulation. As a practical matter, the actual performance in test of the clean rotor (Rotor "A") is clearly superior to that of the repaired Rotor "B" and the computer simulation results themselves are more representative of expected performance from aerodynamically clean rotors. This is borne out by the data presented in Table 1 where the very close correspondence of simulated and experimental results using Rotor "A" is readily apparent.

General Comments

Many of the test runs conducted for the contract were made to ascertain the effect of the seal designs and clearances and used the older Rotor "B" in order to avoid possible damage to the newer Rotor "A". Also, the DU was modified to direct the flow through the reentry exit to the exhaust as shown in Figure 2.

The stronger expansion waves which result from the decreased pressure at the reentry exit port produce a lower residual gas pressure in the wave rotor at a point near the leading edge of the exhaust port. Consequently, the air flow from the scavenge compressor to the wave rotor increases with generally beneficial results to the overall engine process. However, the wave rotor must supply all of the power to drive the scavenge compressor, so that excess scavenge air above 15% is not generally desirable. In the case of the tests conducted for this report, the excess scavenge air flow was about 35% to 45%.

Another consequence of this change is greater absolute Mach number and mass flow at the reentry exit port. Since the GPC DU is configured basically as a gas generator, there is no provision for recovering the proportionately large amount of stagnation enthalpy represented by this flow. The DU was originally designed to include a turbine wheel for this purpose.

With respect to the GPC wave rotor itself, the tangential momentum conditions for gases entering and leaving the rotor are such that positive power is produced at all ports during normal steady-state operation.



1. TITLE		
2. AUTHOR		
3. PERIODICITY		
4. DATE		
5. AVAILABILITY STATEMENT		
6. DISTRIBUTION STATEMENT		
7. AVAILABILITY STATEMENT		
8. AVAILABILITY STATEMENT		
9. AVAILABILITY STATEMENT		
10. AVAILABILITY STATEMENT		
11. AVAILABILITY STATEMENT		
12. AVAILABILITY STATEMENT		
13. AVAILABILITY STATEMENT		
14. AVAILABILITY STATEMENT		
15. AVAILABILITY STATEMENT		
16. AVAILABILITY STATEMENT		
17. AVAILABILITY STATEMENT		
18. AVAILABILITY STATEMENT		
19. AVAILABILITY STATEMENT		
20. AVAILABILITY STATEMENT		
21. AVAILABILITY STATEMENT		
22. AVAILABILITY STATEMENT		
23. AVAILABILITY STATEMENT		
24. AVAILABILITY STATEMENT		
25. AVAILABILITY STATEMENT		
26. AVAILABILITY STATEMENT		
27. AVAILABILITY STATEMENT		
28. AVAILABILITY STATEMENT		
29. AVAILABILITY STATEMENT		
30. AVAILABILITY STATEMENT		
31. AVAILABILITY STATEMENT		
32. AVAILABILITY STATEMENT		
33. AVAILABILITY STATEMENT		
34. AVAILABILITY STATEMENT		
35. AVAILABILITY STATEMENT		
36. AVAILABILITY STATEMENT		
37. AVAILABILITY STATEMENT		
38. AVAILABILITY STATEMENT		
39. AVAILABILITY STATEMENT		
40. AVAILABILITY STATEMENT		
41. AVAILABILITY STATEMENT		
42. AVAILABILITY STATEMENT		
43. AVAILABILITY STATEMENT		
44. AVAILABILITY STATEMENT		
45. AVAILABILITY STATEMENT		
46. AVAILABILITY STATEMENT		
47. AVAILABILITY STATEMENT		
48. AVAILABILITY STATEMENT		
49. AVAILABILITY STATEMENT		
50. AVAILABILITY STATEMENT		
51. AVAILABILITY STATEMENT		
52. AVAILABILITY STATEMENT		
53. AVAILABILITY STATEMENT		
54. AVAILABILITY STATEMENT		
55. AVAILABILITY STATEMENT		
56. AVAILABILITY STATEMENT		
57. AVAILABILITY STATEMENT		
58. AVAILABILITY STATEMENT		
59. AVAILABILITY STATEMENT		
60. AVAILABILITY STATEMENT		
61. AVAILABILITY STATEMENT		
62. AVAILABILITY STATEMENT		
63. AVAILABILITY STATEMENT		
64. AVAILABILITY STATEMENT		
65. AVAILABILITY STATEMENT		
66. AVAILABILITY STATEMENT		
67. AVAILABILITY STATEMENT		
68. AVAILABILITY STATEMENT		
69. AVAILABILITY STATEMENT		
70. AVAILABILITY STATEMENT		
71. AVAILABILITY STATEMENT		
72. AVAILABILITY STATEMENT		
73. AVAILABILITY STATEMENT		
74. AVAILABILITY STATEMENT		
75. AVAILABILITY STATEMENT		
76. AVAILABILITY STATEMENT		
77. AVAILABILITY STATEMENT		
78. AVAILABILITY STATEMENT		
79. AVAILABILITY STATEMENT		
80. AVAILABILITY STATEMENT		
81. AVAILABILITY STATEMENT		
82. AVAILABILITY STATEMENT		
83. AVAILABILITY STATEMENT		
84. AVAILABILITY STATEMENT		
85. AVAILABILITY STATEMENT		
86. AVAILABILITY STATEMENT		
87. AVAILABILITY STATEMENT		
88. AVAILABILITY STATEMENT		
89. AVAILABILITY STATEMENT		
90. AVAILABILITY STATEMENT		
91. AVAILABILITY STATEMENT		
92. AVAILABILITY STATEMENT		
93. AVAILABILITY STATEMENT		
94. AVAILABILITY STATEMENT		
95. AVAILABILITY STATEMENT		
96. AVAILABILITY STATEMENT		
97. AVAILABILITY STATEMENT		
98. AVAILABILITY STATEMENT		
99. AVAILABILITY STATEMENT		
100. AVAILABILITY STATEMENT		

TABLE OF CONTENTS

Technical Discussion	1
Results of Tests and Simulations	7
Recommendations for Further Work	18
List of Symbols	19
List of References	20
Appendix A - Task Summary	21

Technical Discussion

1. Description of Demonstration Unit

The schematic of the GPC DU as arranged for the latest series of tests is shown in Figure 1, and the corresponding port configuration appears in Figure 2. The only noteworthy configuration change concerns the Reentry Exit Ports which are now connected directly to the exhaust duct. They were originally connected to their companion Reentry Nozzle Ports so as to provide two-stage expansion on the wave rotor. However, it was not possible to determine either the true scavenge air flow or the gas flow at Reentry Exit with the original duct arrangement.

With the present port arrangement the residual high pressure air, i.e., the air that is not taken off the rotor at the High Pressure Air Port (state 6, Figure 2) is removed from the wave rotor at the Reentry Exit Port as indicated by the gas-air interface I_2 . Consequently, there is only hot gas remaining on the wave rotor between the trailing edge of the Reentry Exit Port and the leading edge of the Scavenge Air Port. Since the temperature of the hot gas is known as it enters the exhaust duct, the task of determining the excess scavenge air flow is simplified. Also, the flow at the Reentry Exit Port can be varied and more easily measured or calculated.

The Reentry Exit Port flow represents approximately 60% to 75% of the total wave rotor flow and a considerable amount of isentropic gas horsepower even at low rotor speeds. For example, at a combustor gas exit temperature of 1800° F (2260° R), a high pressure air circulation ratio (W_5/W_1) of 0.55 and a rotor speed of 7000 rpm, the isentropic gas power represented by the stagnation enthalpy at the Reentry Exit Port is approximately 4.7 hp. Since the DU is a two-sector engine, this translates to 9.5 isentropic gas horsepower.

The DU, as previously noted and as shown by Figure 1 and Figure 2, is a two-sector wave engine. This means that there are two complete cycles of operation per revolution of the rotor. However, this should not be construed to mean that these are completely independent sectors. That is not dynamically possible because the sectors unavoidably interact at the Scavenge Air and Exhaust Ports. In the case of the DU, the two sectors are also coupled at the high Pressure Ports by a common combustor. This can lead to temperature imbalance in the two Hot Gas Ports because of late burning or from non-symmetrical dilution action. In general this is not a serious operational problem.

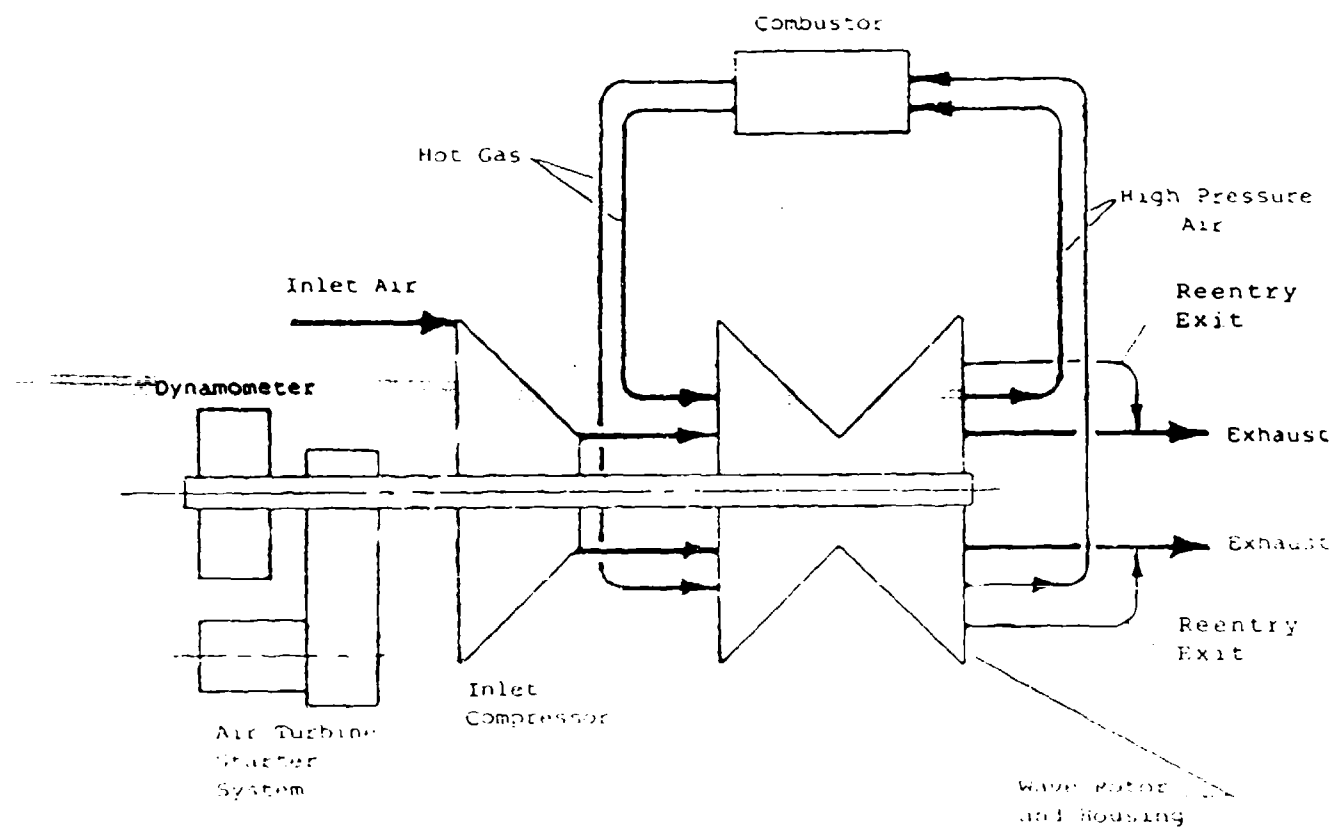


FIGURE 1. GPC WAVE TURBINE SCHEMATIC DIAGRAM

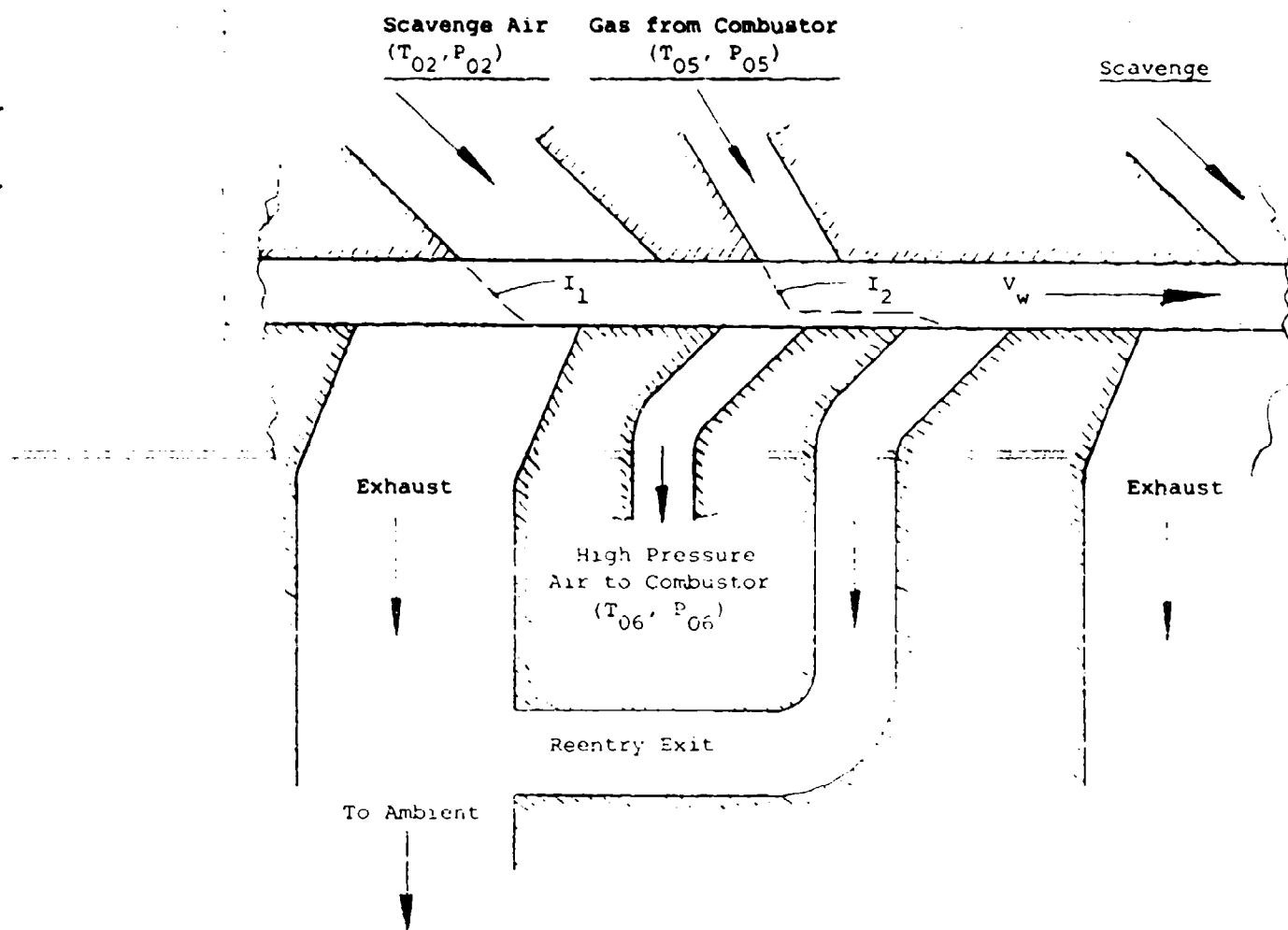


FIGURE 2. GPC DEMONSTRATION UNIT - PORT CONFIGURATION FOR TESTS

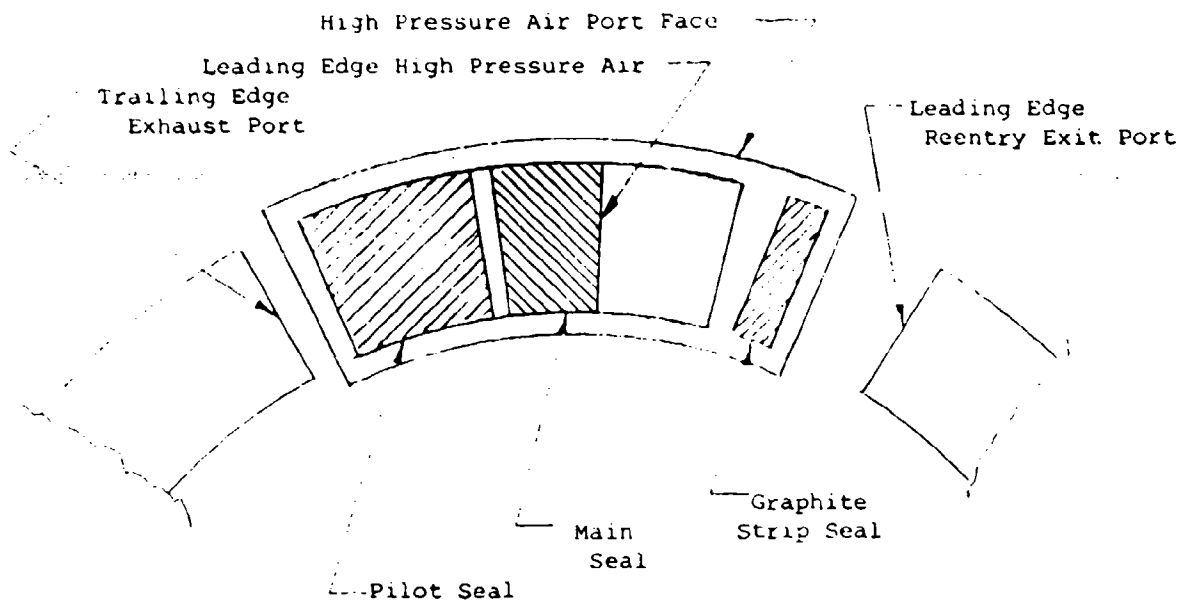


FIGURE 3. SERVO SEAL AT HIGH PRESSURE AIR PORT

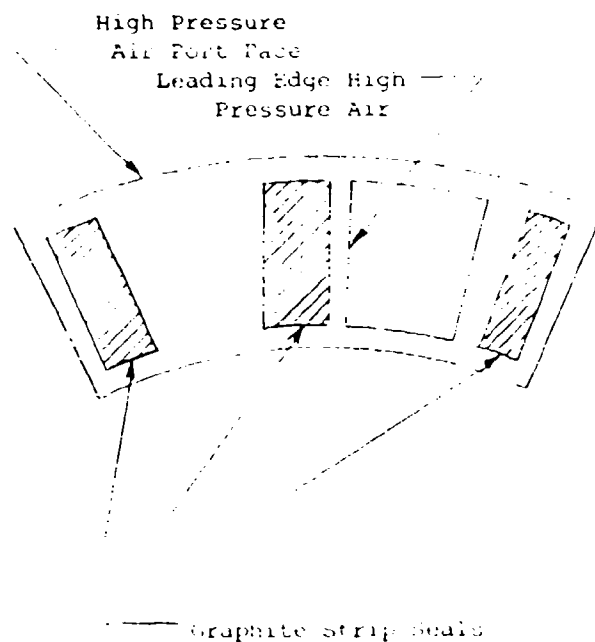


FIGURE 4. ARRANGEMENT OF GRAPHITE STRIP SEALS

Scavenge air is provided by a centrifugal compressor from an old GE Type B aircraft type turbo supercharger. This compressor was designed in the late 1930's and is clearly not representative of modern design techniques. It rarely achieves a measured adiabatic efficiency greater than 64%. The efficiency can be properly accounted for in assessing performance of the DU. However, the lower than optimal pressure rise for a given wave rotor speed causes a diffusing flow (positive angle of attack) at the wave rotor entrance. This condition results in some loss of stagnation pressure and reduction in the pressure ratio of the first wave compression process. The present scavenge compressor will be mismatched with the wave rotor at all speeds. This is not a serious matter, however, except for the reduction in overall pressure ratio of the DU, and can be remedied only by installing another compressor with an impeller having greater diameter or head coefficient, preferably both.

2. Wave Rotor Cavity Seals

Most of the experimental work germane to the contract was devoted to design and clearance adjustment of the face seals and surround seals. Rotor cavity seals have been a source of much trouble with the DU for two principal reasons. First of all, the flame sprayed abrasible seal materials have either been too soft to withstand the erosive action of the hot gases or so hard that they inflict serious damage to the wave rotor in the event of a rub between rotor and stator. Generally, the sprayed nickel-graphite abrasible materials erode rapidly when exposed to gases at temperatures in the neighborhood of 1700°F. It is doubtful that this material will prove to be very useful in the high temperature regions of the GPC Wave Engine. Secondly, the two wave rotors now on hand have thin cross sections in the region between the attachment bolt circle and the base of the blades. Thus, they are susceptible to considerable "dishing" when heated more on one face than the other.

Substitution of mechanically attached graphite seals has helped with both problems. The seal arrangement presently used is shown in Figure 4. Three radially disposed graphite strips are used to impede the angular leakage at the three most critical points on the exit side. Fortunately, all three seals can be located in the face of the High Pressure Air Port block. Use of the radial strip seals made it possible to allow rather large total axial clearances between rotor and casing and then seal off the critical points. The oxidation inhibited graphite used is of medium density and resists gas erosion very well while at the same time wearing without apparent damage to the rotor in the event of rubbing.

The most effective face seal is the one shown in Figure 3. In this arrangement, the pilot seal is closer to the wave rotor face by approximately .002 inches than the main seal. It also operates in a region (state 3 as defined in Attachment D, Reference 1) of near zero angular pressure gradient so that there are practically no angular forces acting on it excepting the viscous drag and bearing forces generated by the velocity of the wave rotor and, of course, the friction force developed during any light contact between the rotor and the pilot seal. Motion of the pilot seal parallel to the direction of rotor rotation allows it to track the relative axial movement of the rotor and also initiate servo action to reposition the main seal to a corresponding new axial location.

This seal arrangement will be the subject of a patent application by GPC in conformance with contract requirements. Consequently, further detailed description of the seal is inappropriate at this time.

3. Computer Simulations

The GPC Wave Engine Simulation Program has been transferred to a microcomputer on the premises at GPC. There were the usual minor but time consuming problems of converting a program to run on a new computer with a new operating system and Fortran compiler. Further, this compiler is structured for the ANSI 77 Fortran which is somewhat different from the compiler provided by the computer utility which GPC previously used.

The simulation program runs on the microcomputer very well indeed, although the computational speed is hardly comparable to that of a large mini or mainframe computer. This particular program requires an enormous amount of computation because of the iterative nature of most calculations and the large number of loopings required to achieve flow balances and to satisfy certain constraints. Other aspects of the computer simulation work have been stated in the summary section. Further indication of the nature of the calculations and the detail revealed by them can be obtained by study of the example given and by the test and simulation results included herein.

Results of Tests and Simulations

The tests of the GPC DU were divided into two general categories. The first series of tests were to ascertain the effects of the aerodynamic improvements in the high pressure air (combustor) loop and the port edge settings which had been incorporated into the DU over a year ago but which had never been tested. The second series of tests were to measure the effect of the new face seals and surround seals with both rotors, one of which (Rotor "B") has an area ratio (A_z/A_y) of approximately .44 and the other (Rotor "A") an area ratio of .50.

Tests indicated that the two-element servo seal increased the High Pressure Air (P_6) to 37.0 psia when used in only one sector compared with approximately 23.6 psia for the abradable seals with runs at nearly the same speed and combustor gas temperature. Only one of these seals was completed and the other is approximately 70% complete. Since time for the program was limited, it was necessary to abandon work on these seals in order to complete the machining and assembly of Rotor "A" and to investigate the performance of the graphite strip seals.

The strip seals, when installed in the face blocks of both High Pressure Air ports, practically duplicated the performance of the single two-element servo seals, producing a pressure of $P_6 = 37.65$ psia when operated with a total axial clearance of .010-.012 inches. This appears to be adequate rubbing clearance. If the clearances are reduced to .006-.008 inches, the rotor will wear the graphite strips but without suffering any apparent damage in doing so.

A performance comparison of the two rotors indicates that the newer rotor (Rotor "A") produces very nearly the same pressure ratio as Rotor "B" at approximately 210°F lower combustor gas temperature but at about the same fuel flow rate. This is directly attributable to the stronger (20% to 25% greater) High Pressure Air circulation produced by the newer rotor. This improved performance is not only a reflection of the cleaner internal flow passages of this rotor but also a consequence of the larger nozzle-to-chamber area ratio.

The remainder of this section will be devoted to a comparison of simulated and actual performance for the conditions:

T_{05} (combustor gas exit) = 1600°F (2060°R);

V_w (rotor pitchline speed) = 350 fps (=7000 rpm);

A_z/A_y (rotor area ratio) = .50;

corresponding to those of data run No. 212.

Printouts of the rotor wave fields and the inlet and exit port conditions have been reproduced in an effort to show the detailed nature of the calculations. It should be noted that the GPC Wave Engine Computer simulation is structured to permit selection of the convergence tolerance for all calculations. It also permits preselection of the minimum level of discontinuity-induced changes in certain variables below which the interactions will be disregarded and other corrections applied. This capability is necessary in order to keep the number of iterations for any port set within reasonable limits. The discussion will make use of Figure 5, the pertinent reproduced printouts and notes, and the following descriptions of the printouts:

Wave Field Out - This is a record of the wave conditions that exist on the rotor at the end of a prescribed region containing one or more ports. These discontinuities are distributed along the y axis.

Wave Field In - This is a record of the wave conditions on the rotor at the beginning of a prescribed region containing one or more ports.

Port Left - Conditions in a port to the left of the rotor for every interaction which occurs at this point from the leading edge to the trailing edge of the port. These interactions are bounded by points along the x axis.

Port Right - Same as above but for a port to the right of the rotor.

Key to the symbols used for the wave field columns are as follows:

(a)	Wave Field Storage Number	
(b)	Location Along x-axis, inches	
(c)	Location along y-axis, inches	
(d)	Slope, dy/dx	
(e)	Pressure Ratio	
(f)	Sonic velocity in gas, ft/sec.	
(g)	Gas velocity, ft/sec.	-to left of discontinuity
(h)	Specific heat ratio	
(i)	Fuel-air ratio	

(j)	Pressure ratio]—to right of discontinuity
(k)	Sonic velocity, ft/sec	
(l)	Gas velocity, ft/sec	
(m)	Specific heat ratio	
(n)	Fuel-air ratio	
(o)	Area change indicator.	

Definitions of column headings for port regions are as follows:

X	Distance from leading edge of port, inches.
U	Gas velocity, ft/sec.
PHI	Angle, degrees with respect to plane of rotation.
MASS	weight flow, lbs/sec.
UX	Velocity parallel to plane of rotation.
UY	Velocity normal to plane of rotation.

The following numbered notes refer to correspondingly marked locations on the reproduced printouts:

- Note 1 - This wave field is synthesized from certain input conditions (bulk properties, as a rule) in order to begin the GPC Wave Engine simulation process.
- Note 2 - The sum of mass flows is calculated by two different methods in the program: either by summation of each state property individually from a particular Wave Field Out, or from continuity conditions on the rotor. Sometimes there are disparities between the two which are resolved as the iteration process continues.
- Note 3 - The average value for Mass Flow On and Mass Flow Off is used to calculate the circulation ratio (W_5/W_A). The pressure drop through the combustor loop of the GPC DE is very low at approximately 7% of maximum flow. Consequently, the simulated stagnation pressure in Port Right (High Pressure Air) may sometimes be lower than stagnation pressure in Port Left (Hot Gas Port) because of the loop balancing tolerance.
- Note 4 - The power produced by the rotor is calculated from these summations and the axial forces are calculated from similar summations.

Note 5 - Notice that Wave Field Out for a previous region becomes Wave Field In for the following region.

Note 6 - Stagnation pressure (P_0) and stagnation sonic velocity (C_0) can be used to calculate the isentropic gas horsepower available at the Reentry Exit Port.

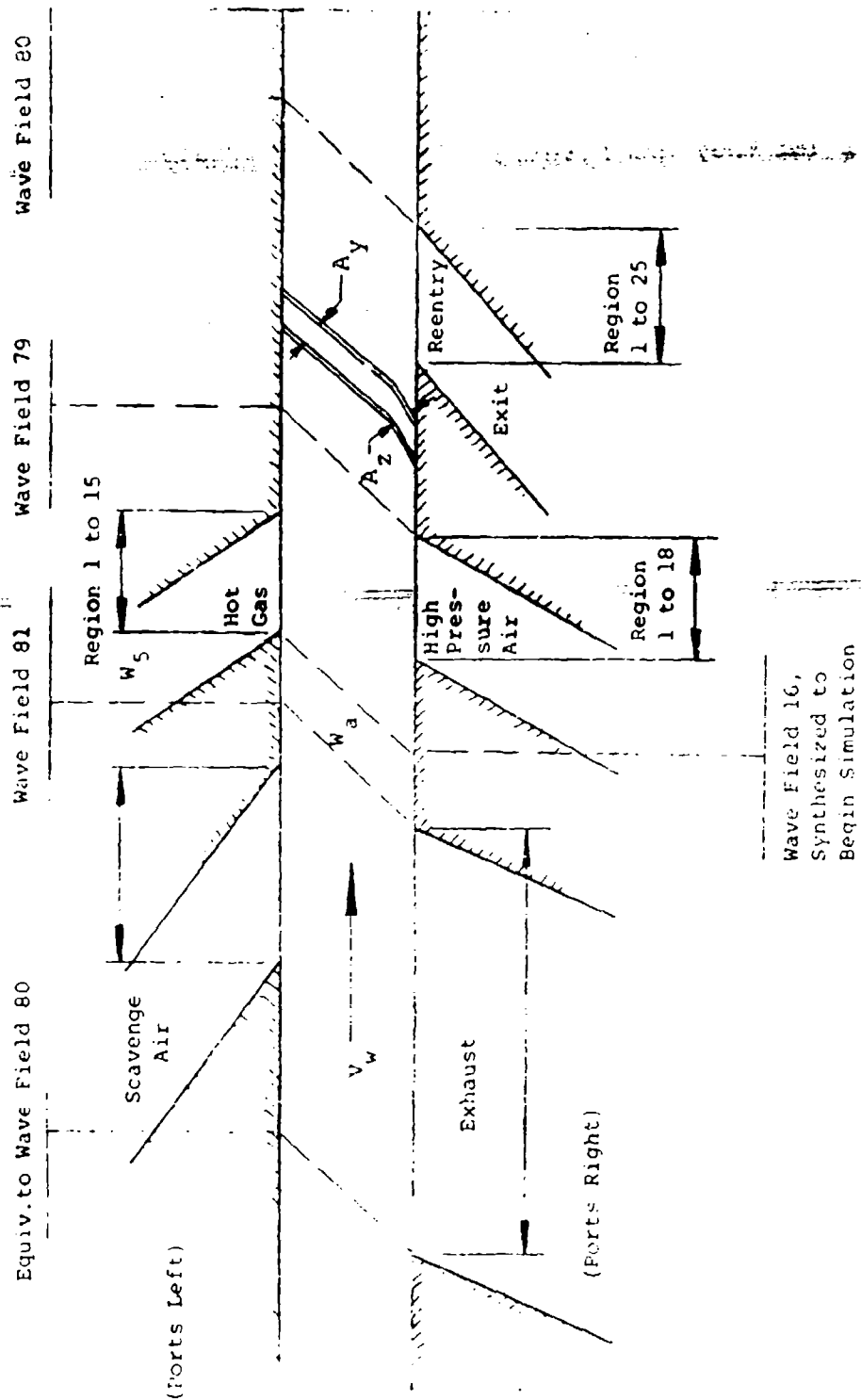


FIGURE 5. LOCATION OF WAVE FIELDS AND PORT REGIONS - GPC WAVE ENGINE SIMULATION (EXAMPLE)

Wave Field 81 and the associated port printouts are not included because they require about four pages since the scavenge air and exhaust ports are relatively long. The printouts contain a total of 125 regions for the two ports, and they add nothing not already revealed in the other sample printouts.

A comparison of the experimental results (Data Run #202) with the simulation for a closely corresponding set of conditions appears in Table 1. There are some disparities because this is an off-design condition. However, it demonstrates the capability of the GPC Wave Engine Simulation Program to predict an idle condition very closely and to show the isentropic gas power available. The speed of the DU varied from 6800 to 7300 rpm during the time required to record the data, but this change has no significant bearing on the results.

GPC WAVE ENGINE SIMULATION - REENTRY EXIT
(Example)

(a)	(b)	(c)	(d)	(e)	(f)	(g)	(h)	(i)	(j)	(k)	(l)	(m)	(n)	(o)	SEC KEY Pages 8 - 9
79	1.991	0.00	0.00	0.00	0.00	0.00	0.00	0.00	0.00	0.00	0.00	0.00	0.00	0.00	0
79	1.991	530	-6.188	3.100	2330.76	321.51	1.316	0.00	2.580	2280.27	321.51	1.316	0.00	0.00	0
79	1.991	611	-5.757	2.580	2280.27	321.51	1.316	0.00	2.727	2295.41	225.62	1.315	0.00	0.00	0
79	1.991	1.215	-6.45	2.727	2295.41	225.62	1.315	0.00	2.726	1379.01	225.62	1.315	0.00	0.00	0
79	1.991	1.281	-3.265	2.726	1379.01	225.62	1.315	0.00	2.626	1371.85	262.30	1.391	0.00	0.00	0
79	1.991	1.349	-3.261	2.625	1371.85	262.30	1.391	0.00	2.720	1382.11	209.71	1.392	0.00	0.00	0
79	1.991	1.547	-6.070	2.720	1382.11	209.71	1.391	0.00	2.196	1337.38	-74.12	1.392	0.00	0.00	0
79	1.991	1.558	-3.743	2.196	1337.38	-74.12	1.391	0.00	2.319	1348.53	-17.25	1.392	0.00	0.00	0
79	1.991	1.603	-3.941	2.319	1348.53	-17.25	1.392	0.00	2.384	1352.91	-39.54	1.392	0.00	0.00	0
79	1.991	1.609	0.00	2.384	1352.91	-39.54	1.392	0.00	2.396	1354.95	-78.63	1.392	0.00	0.00	0
79	1.991	1.615	3.702	2.396	1354.95	-78.63	1.392	0.00	2.423	1357.12	-67.57	1.392	0.00	0.00	0
79	1.991	1.859	5.741	2.423	1357.12	-67.57	1.392	0.00	2.452	1359.38	-56.01	1.392	0.00	0.00	0
79	1.991	1.892	3.799	2.452	1359.38	-56.01	1.392	0.00	2.508	1363.72	-33.82	1.391	0.00	0.00	0
79	1.991	1.926	0.00	2.508	1363.72	-33.82	1.391	0.00	2.603	1382.19	225.00	1.391	0.00	0.00	0

BULK PROPERTIES AT X1=1.991
T=1580.27 P=2.953 C=1852.73

SUM OF MASS FLOWS= 1792

K=1.352

INTERACTION NUMBER= 274
WAVE FIELD OUT HAS ID# = 80

(a)	(b)	(c)	(d)	(e)	(f)	(g)	(h)	(i)	(j)	(k)	(l)	(m)	(n)	(o)	SEC KEY Page 10
79	1.991	0.00	0.00	0.00	0.00	0.00	0.00	0.00	0.00	0.00	0.00	0.00	0.00	0.00	0
79	1.991	530	-6.188	3.100	2330.76	321.51	1.316	0.00	2.580	2280.27	321.51	1.316	0.00	0.00	0
79	1.991	611	-5.757	2.580	2280.27	321.51	1.316	0.00	2.727	2295.41	225.62	1.315	0.00	0.00	0
79	1.991	1.215	-6.45	2.727	2295.41	225.62	1.315	0.00	2.726	1379.01	225.62	1.315	0.00	0.00	0
79	1.991	1.281	-3.265	2.726	1379.01	225.62	1.315	0.00	2.626	1371.85	262.30	1.391	0.00	0.00	0
79	1.991	1.349	-3.261	2.625	1371.85	262.30	1.391	0.00	2.720	1382.11	209.71	1.392	0.00	0.00	0
79	1.991	1.547	-6.070	2.720	1382.11	209.71	1.391	0.00	2.196	1337.38	-74.12	1.392	0.00	0.00	0
79	1.991	1.558	-3.743	2.196	1337.38	-74.12	1.391	0.00	2.319	1348.53	-17.25	1.392	0.00	0.00	0
79	1.991	1.603	-3.941	2.319	1348.53	-17.25	1.392	0.00	2.384	1352.91	-39.54	1.392	0.00	0.00	0
79	1.991	1.609	0.00	2.384	1352.91	-39.54	1.392	0.00	2.396	1354.95	-78.63	1.392	0.00	0.00	0
79	1.991	1.615	3.702	2.396	1354.95	-78.63	1.392	0.00	2.423	1357.12	-67.57	1.392	0.00	0.00	0
79	1.991	1.859	5.741	2.423	1357.12	-67.57	1.392	0.00	2.452	1359.38	-56.01	1.392	0.00	0.00	0
79	1.991	1.892	3.799	2.452	1359.38	-56.01	1.392	0.00	2.508	1363.72	-33.82	1.391	0.00	0.00	0
79	1.991	1.926	0.00	2.508	1363.72	-33.82	1.391	0.00	2.603	1382.19	225.00	1.391	0.00	0.00	0

WAVE FIELD OUT = 80 TO FOLLOW

(a)	(b)	(c)	(d)	(e)	(f)	(g)	(h)	(i)	(j)	(k)	(l)	(m)	(n)	(o)	SEC KEY Page 10
79	1.991	0.00	0.00	0.00	0.00	0.00	0.00	0.00	0.00	0.00	0.00	0.00	0.00	0.00	0
79	1.991	530	-6.188	3.100	2330.76	321.51	1.316	0.00	2.580	2280.27	321.51	1.316	0.00	0.00	0
79	1.991	611	-5.757	2.580	2280.27	321.51	1.316	0.00	2.727	2295.41	225.62	1.315	0.00	0.00	0
79	1.991	1.215	-6.45	2.727	2295.41	225.62	1.315	0.00	2.726	1379.01	225.62	1.315	0.00	0.00	0
79	1.991	1.281	-3.265	2.726	1379.01	225.62	1.315	0.00	2.626	1371.85	262.30	1.391	0.00	0.00	0
79	1.991	1.349	-3.261	2.625	1371.85	262.30	1.391	0.00	2.720	1382.11	209.71	1.392	0.00	0.00	0
79	1.991	1.547	-6.070	2.720	1382.11	209.71	1.391	0.00	2.196	1337.38	-74.12	1.392	0.00	0.00	0
79	1.991	1.558	-3.743	2.196	1337.38	-74.12	1.391	0.00	2.319	1348.53	-17.25	1.392	0.00	0.00	0
79	1.991	1.603	-3.941	2.319	1348.53	-17.25	1.392	0.00	2.384	1352.91	-39.54	1.392	0.00	0.00	0
79	1.991	1.609	0.00	2.384	1352.91	-39.54	1.392	0.00	2.396	1354.95	-78.63	1.392	0.00	0.00	0
79	1.991	1.615	3.702	2.396	1354.95	-78.63	1.392	0.00	2.423	1357.12	-67.57	1.392	0.00	0.00	0
79	1.991	1.859	5.741	2.423	1357.12	-67.57	1.392	0.00	2.452	1359.38	-56.01	1.392	0.00	0.00	0
79	1.991	1.892	3.799	2.452	1359.38	-56.01	1.392	0.00	2.508	1363.72	-33.82	1.391	0.00	0.00	0
79	1.991	1.926	0.00	2.508	1363.72	-33.82	1.391	0.00	2.603	1382.19	225.00	1.391	0.00	0.00	0

WAVE FIELD OUT = 80 TO FOLLOW

(a)	(b)	(c)	(d)	(e)	(f)	(g)	(h)	(i)	(j)	(k)	(l)	(m)	(n)	(o)	SEC KEY Page 10
79	1.991	0.00	0.00	0.00	0.00	0.00	0.00	0.00	0.00	0.00	0.00	0.00	0.00	0.00	0
79	1.991	530	-6.188	3.100	2330.76	321.51	1.316	0.00	2.580	2280.27	321.51	1.316	0.00	0.00	0
79	1.991	611	-5.757	2.580	2280.27	321.51	1.316	0.00	2.727	2295.41	225.62	1.315	0.00	0.00	0
79	1.991	1.215	-6.45	2.727	2295.41	225.62	1.315	0.00	2.726	1379.01	225.62	1.315	0.00	0.00	0
79	1.991	1.281	-3.265	2.726	1379.01	225.62	1.315	0.00	2.626	1371.85	262.30	1.391	0.00	0.00	0
79	1.991	1.349	-3.261	2.625	1371.85	262.30	1.391	0.00	2.720	1382.11	209.71	1.392	0.00	0.00	0
79	1.991	1.547	-6.070	2.720	1382.11	209.71	1.391	0.00	2.196	1337.38	-74.12	1.392	0.00	0.00	0
79	1.991	1.558	-3.743	2.196	1337.38	-74.12	1.391	0.00	2.319	1348.53	-17.25	1.392	0.00	0.00	0
79	1.991	1.603	-3.941	2.319	1348.53	-17.25	1.392	0.00	2.384	1352.91	-39.54	1.392	0.00	0.00	0
79	1.991	1.609	0.00	2.384	1352.91	-39.54	1.392	0.00	2.396	1354.95	-78.63	1.392	0.00	0.00	0
79	1.991	1.615	3.702	2.396	1354.95	-78.63	1.392	0.00	2.423	1357.12	-67.57	1.392	0.00	0.00	0
79	1.991	1.859	5.741	2.423	1357.12	-67.57	1.392	0.00	2.452	1359.38	-56.01	1.392	0.00	0.00	0
79	1.991	1.892	3.799	2.452	1359.38	-56.01	1.392	0.00	2.508	1363.72	-33.82	1.391	0.00	0.00	0
79	1.991	1.926	0.00	2.508	1363.72	-33.82	1.391	0.00	2.603	1382.19	225.00	1.391	0.00	0.00	0

TABLE 1

QUANTITY	SIMULATION	DATA RUN	----- COMMENTS -----
Pressure Ratio P_6/P_A	2.765	2.716	DATA FOR DATA RUN #202
Combustor Temp., T_{05}	1600°F (2060°R)	1561°F (2021°R)	The initial temperature setting of 1600°F changed during the run because of increasing High Pressure Air circulation.
Pitchline Speed, V_w	350 ft/sec	354 ft/sec (avg)	Varies during run. DU is not governed nor does it have automatic fuel flow control.
Rotor Mass Flow, W_A	.2085 lbm/sec	.190 lbm/sec	One Sector Only
Ambient Temp.	70°F (530°R)	80°F (540°R)	Average during run.
Circulation Ratio, W_5/W_A	.414	.52	The simulation loop balance occurred on the low side of the tolerance, resulting in lower mass flow and pressures. The performance of Rotor A is very good.
Mass Flow, Reentry Exit	.1244 lbm/sec	.134 lbm/sec	
Exhaust Flow	.169 lbm/sec	.156 lbm/sec (avg)	
Compressor Flow	.611 lbm/sec	.59 lbm/sec	
Compressor Power	7.685 hp	5.85 hp	Simulations indicate higher ΔT than measured.
Power at Scavenge and Exhaust	2.126 hp	-	
Power at High Pressure Port	1.408 hp	-	
Power at Re- entry Exit	3.835 hp	-	
Total Rotor Power	7.369 hp	-	
Net Power	-.316 hp	0.1	
Isentropic Gas Power at Re- entry Exit	9.343 hp	-	Instrumentation does not permit accurate measurement of this.
Fuel Flow (18,400 BTU/lb)	12.87 lb/hr	13.38 lb/hr	

Recommendations for Further Work

1. Upgrade of the GPC Demonstration Unit to a high performance test unit by doing the following:

- a. Design and fabricate new rotors of the type shown on page 72 of Reference 1. This rotor type would employ a dual disk for axial stability and have cast blades attached to the disk by some mechanical means. The blades themselves would be designed in accordance with analysis of Attachment D, pages 51-71, Reference 1.
- b. Modify the DU to accept dual combustors which could be operated at exit gas temperatures in the neighborhood of 2400°F (2860°R).
- c. Replace the present scavenge compressor with one of modern design that can produce a pressure ratio of 3.5 at 24,000 rpm.
- d. Continue development work on the face seals and surround seals along lines begun during the present contract.
- e. Design and construct high performance power turbines for operation on same shaft as DU, or as separate free turbines.

2. Conduct experimental and theoretical work on such topics as:

- a. Gas interface mixing.
- b. Port opening and closing dynamics.
- c. The work as set out in proposals of Reference 1.

LIST OF SYMBOLS

- A_y - Flow area of wave rotor chamber, i.e. the area defined by the normal distance between two adjacent blades multiplied by the radial blade height at any axial location between the rotor entrance plane and the beginning of the nozzle transition.
- A_z - Flow area of wave rotor nozzle, i.e. the area defined by the normal distance between two adjacent rotor blades multiplied by the radial blade height at the end of the nozzle transition.
- I_1 - Air-gas interface established during low pressure scavenge process. By definition, the static pressures of the gases on opposite sides of the interface are equal and so are the gas velocities.
- I_2 - Gas-air interface established during high pressure energy exchange and compression process.
- P_{0n} - Stagnation pressure at location n.
- T_{0n} - Stagnation temperature at location n.
- W_a - Weight of air per unit time on wave rotor at completion of low pressure scavenge and first stage wave compression processes.
- W_s - Weight of gas per unit time entering wave rotor at Hot Gas Port. Same as weight flow of air leaving rotor at High Pressure Air Port, except for the fuel added during combustion.

LIST OF REFERENCES

1. Coleman, Richard R., GPC Wave Engine Technology, Status Summary and Analyses, with additions and revisions of 8-18-83.
2. Work Statement included with proposal of December 7, 1982.
(See copy, Appendix A).

APPENDIX A

TASK SUMMARY

- I.1 Prepare and Test Engine with Rotor 'b', Area Ratio = .46.
 - I.2 Prepare and Test Engine with Rotor 'a', Area Ratio = .50.
 - I.3 Prepare and Test Engine with Improved Rotor Seal Configuration and Rotor 'a'.
 - II.1 Simulation Support for Test.
 - II.2 Test Data Reduction and Correlation with Simulation Data.
 - III. Final (and Quarterly) Report.
-

END

DATE
FILMED

4-84

DTIC